THEORETICAL AND APPLIED MECHANICS
Volume 47 (2020) Issue 1, 33–62 DOI: https://doi.org/10.2298/TAM200117004R

AN OVERVIEW OF APPLICATION OF MICROMECHANICAL MODELS IN DUCTILE FRACTURE ANALYSIS OF WELDED JOINTS

M. Rakin, B. Medjo, N. Gubeljak, and A. Sedmak

Abstract. Fracture of welded joints has been an important research and industrial topic for a long time, having in mind the key role of welded joints in ensuring the safe operation and integrity of welded structures. This work contains an overview of application of micromechanical models to ductile fracture of welded joints. The main benefit of these models, in comparison with the classical fracture mechanics approach, is consideration of the local quantities (stress and strain) in prediction of damage development. The damage is quantified through the value of the damage parameter, which is typically related to the void nucleation, growth and coalescence for ductile fracture of metallic materials, i.e. the description of the material can be related to the actual material behaviour during fracture. Most of the presented studies, including those published by the present authors, are performed on steel as the base material, and the rest deal with aluminium alloys.

1. Introduction

1.1. Fracture of welded joints. Welding is one of the most common techniques for joining metallic materials. There are numerous books, publications and journals dealing with different aspects of production, exploitation and integrity assessment of welded structures, e.g. [**1**, **2**]. Steel and aluminium alloys have been dominant construction materials for welded structures in many industries for a long time. However, other materials have also found an increasing application more recently, some of which are also often joined by welding (e.g. magnesium, copper or titanium alloys), [**3**,**4**]. In addition, welding is used as a joining method in the field of polymer materials and polymer composites, [**5**, **6**].

The process of welding typically causes different types of inhomogeneities in the region of the welded joint. Some of the causes are the heat input during

2010 *Mathematics Subject Classification:* 74R20.
Key words and phrases: micromechanical models, welded joint, fracture initiation and development, mismatch.

welding, cooling regime and differences in mechanical/microstructural properties of the base metal and filler material. Inhomogeneities at the micro level, such as micro-cracks, inclusions or pores, can develop to a macro-defect and pose a threat to the safe service of the welded structure. Additionally, macroscopic inhomogeneity (difference in tensile and other properties of the joint zones) influences further development of the crack through the joint. Depending on the material properties, loading conditions, but also exploitation conditions, failure mechanisms of welded structures can be different: brittle or ductile fracture, fatigue, plastic collapse or their combination. In this work, we focus on ductile fracture.

In metals and alloys, the ductile fracture mechanism occurs through void nucleation, growth and coalescence. Voids typically nucleate around some inhomogeneities in the material, such as inclusions. Depending on the properties of the particle and the material (typically, the term *matrix material* is used), a void can be created by particle fracture or debonding of the particle from the matrix. Once nucleated, the void represents the stress and strain concentration region, and it will grow when some external loading is present. It is important to emphasize the local nature of this phenomenon, i.e. local damage development, which does not depend on the geometry of the structure.

At some point, multiple voids in the material have grown significantly under external loading and the ligament between them becomes thinner. This ends in the coalescence (joining) of the neighbouring voids, through localization of plastic deformation in the ligaments between them. This process can be seen in microphotographs of fracture surfaces of components or specimens failed by the ductile fracture mechanism, where some of the dimples contain inclusions around which the voids have been nucleated. Authors of the review article [**7**] gave a comprehensive overview of both ductile and brittle fracture of metallic materials.

1.2. Constraint and mismatch effects. The constraint effect has an important role even in macroscopically homogeneous materials; the factors which influence the constraint are considered by many authors, e.g. [**8**, **9**]. In welded joints, the influence of material heterogeneity or mismatch is additionally present.

Regarding the strength of welded joints, they are typically categorised into undermatched, overmatched or evenmatched (UM, OM and EM). This basic categorisation takes into account only the yield strength of the base metal and the weld metal, without taking deformation hardening into consideration, and it is quantified through the mismatch ratio M. A rather simplified view on the influence of material heterogeneity on welded joints with cracks can be given through the plastic zone shape, Figure 1. However, a detailed analysis should also include different hardening properties of the weld metal zones; this is taken into account in micromechanical analysis, because the modelling is based on the true stress–true strain curves.

A very good collection of studies dealing with mismatch effects on fracture of welded joints and interfaces is found in the conference proceedings [**11**], edited by Schwalbe and Kocak in 1997. Many aspects are covered: experimental determination of fracture mechanics parameters and fracture toughness, analytical and

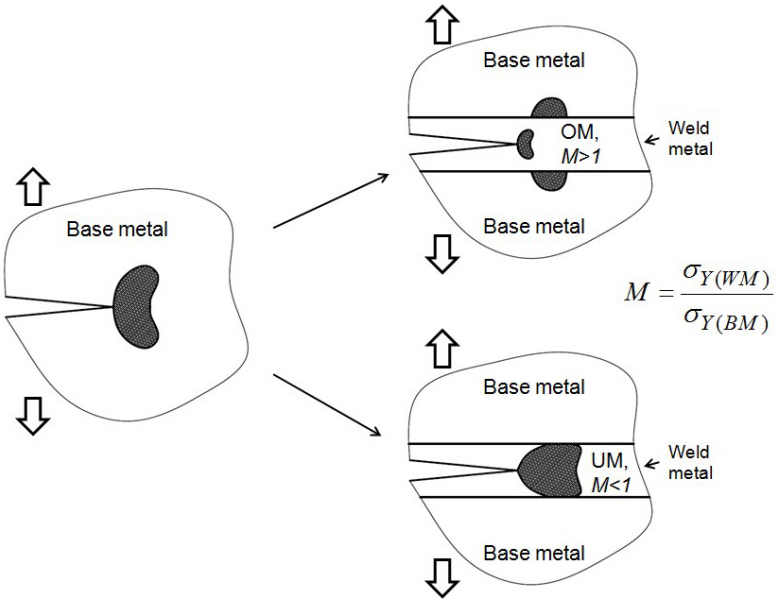

FIGURE 1. Influence of undermatching and overmatching on the plastic zone shape in welded joints, based on [**10**].

numerical analysis of stress state in the crack tip region, determining the yield loads, fracture of dissimilar joints, etc. In this publication, one of the chapters, [**12**], deals with the influence of mismatch (mismatch correction) on determination of fracture mechanics parameters and structural integrity assessment of welded structures. Nearly simultaneously with this publication, Schwalbe et al. developed and published the procedure EFAM ETM-MM [**13**], for the assessment of the significance of crack-like defects in mismatched joints.

Application of fracture mechanics parameters (often referred to as the global approach to fracture) is typically related to the problem of parameter transferability. This is a problem which is not related only to heterogeneous materials, such as joints, but also exists in macroscopically homogeneous ones. The authors of [**12**] describe this issue related to the crack tip constraint in this way: one fracture mechanics parameter is not sufficient for linking the fracture behaviour between the specimens and engineering components/structures. Contrary to this, the ductile fracture mechanism itself does not depend on the geometry of the structure, as previously mentioned.

In the literature, there are different attempts to overcome this problem through introducing additional parameter(s) to improve the prediction of fracture resistance by using the fracture mechanics methodology. This resulted in proposals of several methods which are often referred to as two-parameter fracture mechanics. An additional parameter is typically related to the level of constraint, and some of the proposed methods are: J–h, J–T, J–Q, J–A_2. The main aim is to quantify

the dependence of fracture behaviour on the geometry of both the structure and the crack. We mention three studies here [**14**–**16**] which contain the application of this concept to welded joints, by introducing both the second and third parameter related to constraint and mismatch effect, respectively.

As mentioned previously, two-parameter fracture mechanics and similar methods introduce some additional parameter(s) (such as triaxiality, or T-stress) in order to quantify the constraint effect. On the other hand, if the local approach is applied in fracture analysis, the constraint is a natural outcome of the damage development in the material, obtained through the use of micromechanical models.

Recent review articles [**17**–**19**] summarise the application of different fracture mechanics methods to welded joints. These reviews cover many topics, from experimental examination of the joints to analytical determination of the crack driving forces in welded components. Due to different loading conditions which act on the welded structures and components, different fracture mechanisms are covered, the main ones being fracture and fatigue. Fatigue of weldments, which is often the dominant failure cause of dynamically loaded structures, is considered in [**20**].

In this work, quasi-static loading and ductile fracture mechanism of welded joints are covered. Micromechanical models of the local approach to fracture have been applied in the analysis of fracture of welded joints in many studies. Some of the main aspects are summarised and commented on in this work.

2. Micromechanical models of the local approach to fracture

The local approach to fracture is a rather wide area, comprising models and methods for the assessment of ductile fracture, cleavage, combined mechanism, etc. An often mentioned advantage of the local approach and micromechanical modelling, in comparison with the global or classical approach of fracture mechanics, is the ability to describe the fracture mechanism in accordance with the material behaviour at the local level. The main aim is to achieve *transferability* of the model parameters to different geometries, by using a combined numerical-experimental procedure which typically includes material characterisation, fracture mechanics testing, microstructural and numerical analysis.

Micromechanical models for the analysis of ductile fracture can be categorised into two main groups: uncoupled and coupled. The difference is based on the treatment of voids. In the first group, the growth of a single void is analysed, and the damage parameter is not included in the constitutive relation. The second group, which is much more used nowadays, treats the material as a continuum which is 'weakened' by the voids. Only a few basic equations for the selected micromechanical models are given here, while a detailed overview can be found in the review works which deal with this topic, e.g. [**21**, **22**]. In these review articles, the authors (Besson [**21**] and Benzerga et al. [**22**]) covered many different aspects of development and application of the models, including anisotropy, void coalescence, void nucleation, etc. In another review article [**23**], Pineau gave a general overview of the development of the local approach to fracture up to 2006, considering both ductile and brittle fracture mechanisms.

2.1. Uncoupled approach. The models which belong to this approach are sometimes referred to as void growth models. From this group, the Rice and Tracey model [**24**] has been used rather often. Actually, one of its modifications is probably most often used – this modification was proposed by the Beremin research group [**25**]:

$$\ln\Big(\frac{R}{R_0}\Big) = 0.283 \int_0^{\varepsilon_{eq}^p} \exp\Big(\frac{3}{2}\frac{\sigma_m}{\sigma_{eq}}\Big) d\varepsilon_{eq}^p \tag{2.1}$$

The damage parameter here is the void growth ratio R/R_0, and it represents the ratio of the mean void radius (at a particular time/loading), while R_0 is the initial radius. In this expression, two very important quantities, which are present in almost all micromechanical models, can be seen: stress triaxiality σ_m/σ_{eq} (ratio of the mean and equivalent stress) and equivalent plastic strain ε_{eq}^p. Since this model deals with the growth of the voids, and the coalescence is not included, a criterion which defines the coalescence (as the third and final stage of ductile damage development) must be introduced. In [**25**], the critical value of the void growth ratio is formulated:

$$\ln\Big(\frac{R}{R_0}\Big)_c = 0.283 \int_0^{\varepsilon_f} \exp\Big(\frac{3}{2}\frac{\sigma_m}{\sigma_{eq}}\Big) d\varepsilon_{eq}^p$$

For application of this criterion, it is necessary to determine σ_f – strain at fracture.

In [**26**], Hancock and Mackenzie proposed a simplified version, called the stress modified critical strain or SMCS model. According to their proposal, the criterion for initiation of ductile fracture is based on reaching the critical value of the plastic strain, which depends on the stress state:

$$\varepsilon^p > \varepsilon_c^p = \alpha \exp\Big(\frac{3}{2}\frac{\sigma_m}{\sigma_{eq}}\Big)$$

The authors of [**26**] propose determining the material-dependent parameter α based on the testing of the notched tensile specimens. The SMCS model is used in several studies of ductile fracture of welded specimens and structures presented in the following two sections.

Huang [**27**] defined different damage development for different triaxiality values and proposed the following expressions:

$$\ln\Big(\frac{R}{R_0}\Big) = 0.427 \int_0^{\varepsilon_{eq}^p} \Big(\frac{\sigma_m}{\sigma_{eq}}\Big)^{1/4} \exp\Big(\frac{3}{2}\frac{\sigma_m}{\sigma_{eq}}\Big) d\varepsilon_{eq}^p \quad \text{for } \sigma_m/\sigma_{eq} \leqslant 1$$

$$\ln\Big(\frac{R}{R_0}\Big) = 0.427 \int_0^{\varepsilon_{eq}^p} \exp\Big(\frac{3}{2}\frac{\sigma_m}{\sigma_{eq}}\Big) d\varepsilon_{eq}^p \quad \text{for } \sigma_m/\sigma_{eq} > 1$$

Dung proposed an uncoupled model which takes into account the ellipsoidal shape of the voids [**28**]:

$$\ln\frac{R_1}{R_0} = \int_0^{\varepsilon} \Big\{ \Big[\frac{\sqrt{3}}{(1-n)} \sinh\Big(\frac{\sqrt{3}\cdot(1-n)}{4} \frac{3\cdot\sigma_m}{\sigma_{eq}} \Big)$$

$$\cosh\left(\frac{\sqrt{3}\cdot(1-n)}{4}\frac{\sigma_2-\sigma_3}{\sigma_{eq}}\right)\Bigg] + \frac{6}{4}\frac{\sigma_1-\sigma_2-\sigma_3}{\sigma_{eq}}\Bigg\}d\varepsilon$$

In this equation, n is the hardening exponent, R_1 is the void semi-axis in straining direction, while R_2 and R_3 would be semi-axes perpendicular to this direction (the same meaning of indices is used for stress values σ_1, σ_2, σ_3), [**28**].

The work by Chaouadi et al. [**29**] contains a different damage parameter instead of the void growth ratio – the damage work. Another model which is formulated based on energy is proposed by Wang in [**30**] – based on damage accumulation.

An interesting proposal is given in [**31**] by Dutta and Kushwaha; they integrated the Rice–Tracey expression across the process zone around the crack tip. In this way, they present the prediction of the fracture mechanics parameter (J integral) at crack growth initiation which is almost independent of the finite element size.

Some of the studies of ductile fracture mentioned in the next section belong to the group of uncoupled models, which proves that they can be successfully used despite the fact that more research efforts have recently been devoted to the models of coupled approach.

2.2. Coupled approach. As mentioned previously, coupled models incorporate the damage parameter into the constitutive equation, i.e. occurrence and development of the damage in the material influence yielding. The variable which is most often used as the damage parameter is void volume fraction or porosity f. This group of models has been developed and modified for several previous decades, and most of such studies (i.e. developed/modified models) are based on the works by Rousselier [**32**] or Gurson [**33**].

The model proposed by Rousselier [**32**] has the following form:

$$\phi = \frac{\sigma_{eq}}{1-f} + Df\sigma_K \exp\left(\frac{\sigma_m}{\sigma_K(1-f)}\right) - \sigma = 0$$

σ is the current flow stress of the material matrix, σ_m is the mean stress, σ_{eq} is the von Mises equivalent stress, D is the material-independent constant, while σ_K is the material-dependent constant. The Rousselier model is used in several studies dealing with welded joint fracture which are mentioned in the next sections.

The Gurson model, published in [**33**], has been the basis for a lot of subsequent modifications, and probably the most often used one is proposed by Tvergaard and Needleman [**34**, **35**]. In the literature, this model is known as GTN or Gurson–Tvergaard–Needleman model:

$$\phi = \frac{3S_{ij}S_{ij}}{2\sigma^2} + 2q_1 f^* \cosh\left(\frac{3q_2\sigma_m}{2\sigma}\right) - [1 + (q_1 f^*)^2] = 0$$

S_{ij} is the stress deviator, q_1 and q_2 constitutive parameters, and f^* is the damage function, or modified void volume fraction:

$$f^* = \begin{cases} f & \text{for } f \leqslant f_c \\ f_c + K(f - f_c) & \text{for } f > f_c \end{cases}; \quad K = \frac{f_u^* - f_c}{f_F - f_c} \tag{2.2}$$

K is the parameter that represents the loss of load-carrying capacity of the material due to the ductile fracture development. The value of the damage function at the moment of fracture is denoted as $f_u^* = 1/q_1$, while the void volume fraction at final fracture is denoted as f_F. A crucial parameter is the critical void volume fraction at void coalescence, denoted as f_c. After this value is reached, the damage development accelerates, in accordance with Equation (2.2).

The increase in the void volume fraction has two components: the first one coming from the growth of the existing voids, and the second one which represents the nucleation of the new (often called secondary) ones during the increase in loading:

$$\dot{f} = \dot{f}_{\text{nucleation}} + \dot{f}_{\text{growth}} \tag{2.3}$$
$$\dot{f}_{\text{nucleation}} = A\dot{\varepsilon}^p_{eq}$$
$$\dot{f}_{\text{growth}} = (1-f)\dot{\varepsilon}^p_{ii}$$

where A is the void nucleation rate, $\dot{\varepsilon}^p_{eq}$ is the equivalent plastic strain rate and $\dot{\varepsilon}^p_{ii}$ is the plastic part of the strain rate tensor. One of the rather often used ways to formulate the void nucleation rate is given by Chu and Needleman [**36**]:

$$A = \frac{f_{\text{N}}}{S_{\text{N}}\sqrt{2\pi}} \exp\Big[-\frac{1}{2}\Big(\frac{\varepsilon^p_{eq} - \varepsilon_{\text{N}}}{S_{\text{N}}}\Big)^2\Big] \tag{2.4}$$

In this expression, f_N is the volume fraction of void nucleating particles, ε_N is the mean strain for void nucleation and S_N is the standard deviation. Equation (2.4) is not the only way to describe the nucleation of voids. Two other methods are applied in [**37**, **38**], where it is either assumed that all the voids are nucleated simultaneously, or they are nucleated at a constant rate during the increase in loading.

Another modification of the Gurson model is proposed by Zhang et al. – the Complete Gurson model, [**37**,**39**]. The main change introduced is the consideration of the criterion of the onset of void coalescence. This criterion, Equation (2.5), takes into account the plastic limit load model proposed by Thomason [**40**], adding it to the initial expressions for the GTN model. The main idea of this, and some other models which deal with the coalescence of voids, is change of the deformation mode – homogeneous to localised (in the intervoid ligaments).

$$\frac{\sigma_1}{\sigma} > \left(\alpha\Big(\frac{1}{r} - 1\Big) + \frac{\beta}{\sqrt{r}}\right)(1 - \pi r^2) \text{ where } r = \sqrt[3]{\frac{3f}{4\pi}e^{\varepsilon_1+\varepsilon_2+\varepsilon_3}} \Bigg/ \left(\frac{\sqrt{e^{\varepsilon_2+\varepsilon_3}}}{2}\right) \tag{2.5}$$

In Equation (2.5), σ_1 is the maximum principal stress, r is the void space ratio, ε_1, ε_2 and ε_3 are principal strains, while α and β are constants fitted by Thomason [**40**] to the values 0.1 and 1.2, respectively. A slightly different approach is applied in CGM; Zhang et al. [**37**] introduced a linear dependence of α on n (hardening exponent).

There are also some published works which deal dominantly with the coalescence stage of ductile fracture, like Pardoen and Hutchinson [**41**] and Zhang [**42**]. Other aspects included in the modifications of the GTN model by different authors

include the anisotropy of plastic properties of the material, [**43**], or non-spherical shape of the voids [**44**, **45**].

Some of the relatively recent works include the effect of shear loading on ductile damage development, such as [**46**, **47**]. Application of these models in fracture analysis of welded joints is mentioned in the following text.

More details about different models of the coupled approach can be found in the original works, and also in the previously mentioned review papers [**21**, **22**].

Micromechanical models of the local approach to fracture have been successfully applied for several decades in fracture analysis of a wide range of materials and structures. As mentioned previously, transferability of parameters between different geometries is one of their main advantages over the global or classical fracture mechanics approach. On the other hand, a drawback is dependence of the results on the finite element mesh, i.e. existence of the *characteristic distance* for the considered material. In many studies, it is said that a relation exists between the appropriate finite element size and material microstructure, expressed through the mean free path between the particles (inclusions, etc.) λ. Therefore, the mesh-dependence problem is typically solved by treatment of the FE size as one of the material parameters; once determined, it can be transferred to the other geometries produced from the same material. The non-local models represent another possible solution. However, in addition to their increased complexity, it is still necessary to determine the characteristic distance (it is used as an internal parameter instead of defining the element size).

3. Application of micromechanical models in fracture analysis of welded standard specimens

In the paper [**48**], published in 1989, critical void growth ratios $(R/R_0)_c$ for two steel weld metals are analysed by considering spherical inclusions with different size distributions. The determination of the critical void growth ratio is performed experimentally – based on the analysis of the fracture surfaces by scanning electron microscopy. Dimples are considered as voids at the moment of fracture, while measures of inclusions at their bottoms are used for the initial void size. It should be mentioned that direct measurement of the critical void growth ratio on fracture surfaces is not often applied in the literature, which is one of the reasons for mentioning this particular paper here. Low dependence of the critical void growth ratio on stress triaxiality is obtained for the considered weld metals. This should not be generalised because interdependence of these quantities (more or less pronounced) has been reported in the literature for different materials. The authors of [**48**] also state that the critical void growth ratios determined by the Rice–Tracey model are lower in comparison with the values obtained by direct measurement, mentioning a possibility to treat the constant in the Rice–Tracey model as a material-dependent parameter instead of the constant value 0.283 given by Equation (2.1).

In another early study, from the point of view of the local approach application to welded joints, Al Rasis et al. [**49**] applied the Rice–Tracey model in the analysis of stainless steel joints. The fracture of compact tension (CT) specimens was

considered, and three zones were modelled: weld metal, base metal and heat affected zone. The specimens' configurations were: BM only, BM + WM and BM + WM + HAZ. In addition to the prediction of fracture initiation in these geometries, the authors simulated the crack growth, but not in the welded joint (this part of the study was not performed on the entire joint). For this purpose, the node release technique was applied; the authors showed that the slope of the crack growth resistance curve (dJ/da) was predicted well, but the values of J integral were lower than in the experiment.

The authors of **[50]** applied both the uncoupled and coupled approach, i.e. micromechanical models of Rice and Tracey and Rousselier in fracture analysis of C–Mn steel welded joints. The compact tension specimens consisted of three materials, and the initial crack was positioned in HAZ; the experiments were conducted at elevated temperature, 300 °C, because the material is used for components of a pressurised water reactor. The main concern was the influence of the micromechanical parameters on the crack growth resistance curves. Also, the influence of the FE size was examined. Due to the different definition of the damage parameter in the applied models, different techniques were used for crack growth modelling – node release for the Rice–Tracey model and damage tracking in the elements for the Rousselier model; two-dimensional plane strain conditions were applied. In the analysed models with three materials, the authors conclude that the second approach gave better results, because significant crack path deviation is observed, Figure 2. In addition, an estimate of the crack path deviation is given based on the value of (R/R_0) in different directions in front of the crack tip; this approach is also mentioned in **[49]**.

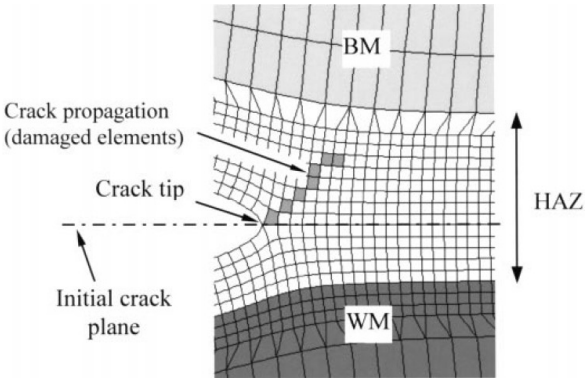

FIGURE 2. Crack path in the heat affected zone, Rousselier model, **[50]**.

Another model of the uncoupled approach, obtained as a modification of the Rice–Tracey model, is applied in a recent work **[51]** to structural steel welded joints. The authors refer to the developed model as the "three-stage and two-parameter ductile fracture model". Flat specimens are examined, and also those with a notch-type stress concentrator with U and V shape (the radius of the U-shaped notch was

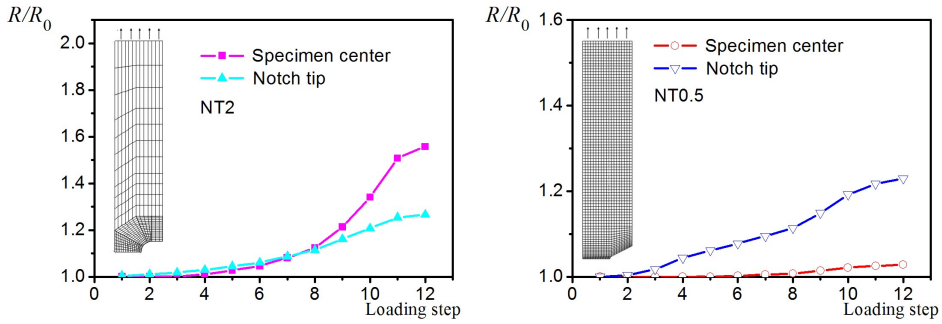

FIGURE 3. Cylindrical notched tensile specimens NT2 (a) and NT 0.5 (b) – damage parameter R/R_0 at the specimen centre and at the notch tip.

2 mm). For the notches positioned in HAZ, the position is varied, so the notch tip was positioned either in the middle of HAZ or near the boundaries HAZ/WM and HAZ/BM. Also, the mesh sensitivity analysis is performed, based on the influence of the finite element size on the load-displacement curve. Significant influence of mesh on the fracture behaviour is obtained for the V-notched specimens (which makes sense, due to the higher stress gradients), and in the case of pre-cracked geometries it is expected to be even more pronounced. On the other hand, the results obtained on U-notches do not show a significant influence of the FE size. The topic of mesh sensitivity for non-crack stress concentrators will be mentioned once more in this work, in the next section.

However, there is another aspect to be considered in the notched specimens (here, it will be shown on the example of a different material – pressure vessel steel): the influence of the notch radius on the predicted fracture initiation position. The Rice–Tracey model is applied, and the damage parameter R/R_0 is tracked at the notch tip and at the centre of the cylindrical notched specimens with notch radii 2 mm and 0.5 mm (NT2 and NT0.5). Of course, both specimens exhibit stress and strain concentration due to the notch existence, but more pronounced damage development is predicted at the notch tip only for smaller radius, Figure 3; for the notch radius 2 mm, the damage develops more rapidly in the specimen centre, like in the smooth cylindrical specimen.

Some other examples of the application of uncoupled models will also be given in the next section.

The Rousselier micromechanical model [**32**] is applied by Burstow and Howard [**14**] to simulate the crack growth in steel welded joints with different levels of mismatching. In this work, the authors applied the two-parameter fracture mechanics approach in combination with the micromechanical model, in order to determine the combined influence of constraint due to the heterogeneity and T-stress. The same model is also applied in [**52**] in fracture analysis of Al6061 alloy laser welded

joints. The fracture behaviour of the base metal and fusion zone is assessed by testing the CT specimens. The micromechanical parameters are determined through a combination of metallographic examinations and notched tensile specimens testing (fitting procedure). This work is characteristic because the fusion zone of the weld is rather narrow – around 1.5 mm, which means that the fusion lines are very close to the crack tip. The authors reported a good prediction of fracture behaviour for different crack positions in the considered welds. Another study, by almost the same group of authors, dealing with very narrow joints, is **[53]**, where fracture of S355NL steel electron beam welded joints is examined. In comparison with the previous work, another position for the initial crack is added, on the interface between the fusion zone and the heat affected zone. The initial porosity (applied in the Rousselier model) is determined from metallographic examination, i.e. it is set equal to the volume fraction of inclusions. The mean free path is also measured this way and initially used as the characteristic distance, but additional calibration is also performed based on the testing of the notched specimens. It should be mentioned that the authors observed a high level of heterogeneity within HAZ, so it is divided into three sub-zones. The fusion zone exhibited brittle behaviour, so it was not included in the micromechanical fracture analysis; as mentioned previously, the Rousselier model is for ductile fracture.

In order to capture and predict the mismatch effect, Lin et al. analysed the ductile fracture of an undermatched interleaf exposed to tensile loading in **[54]**. An undermatched joint is selected due to the fact that the plastic deformations (Figure 1) and triaxiality can become rather high and confined to a small volume of material in such configurations. The authors assumed that no voids were initially present in the material in the unloaded state ($f_0 = 0$); in the micromechanical analysis by using the GTN model, all the voids were nucleated during the loading increase, in accordance with Equation (2.4). Stress and strain state, as well as damage parameter fields were analysed in detail in 2D plane strain conditions, on a middle-cracked tensile plate. Special consideration was devoted to the mean stress and plastic strain, as key quantities for ductile fracture process, Section 2. For the considered material properties, the authors concluded that the thickness of the undermatched material did not influence the prediction of crack initiation, while the crack growth resistance was affected and decreased for smaller thickness.

Li et al **[55]** applied the same model in analysis of fracture of steel welded joints. Two different steels were used as base metals in this study. Unlike most of the other studies dealing with fracture behaviour of welded joints, specimens without an initial crack or stress concentrator were considered (micro tensile specimens with rectangular cross section), i.e. the initiation of ductile fracture in low-triaxiality conditions was the main concern. The authors of **[55]** introduced a new term into the expression for void volume fraction rate determination, thus obtaining a different measure of damage – f becomes "the void volume fraction of inactive material". Based on the results of the micromechanical analysis, they propose the use of wider joints in case of UM, while more narrow joints have better fracture resistance for OM joints.

In [**56**], Rakin et al. presented an analysis of the pre-cracked high strength steel welded joints (the base metal was NIOMOL 490). The analysis included overmatched and undermatched welded joints with different width $2H$ (6, 12 and 18 mm), Figure 4. The development of damage in front of the pre-crack and initiation of ductile fracture were the main concern of this work, along with determining the influence of the joint width on the crack growth onset. In the framework of the GTN model, the critical value of the damage parameter (f_c) is transferred from the round tensile specimens cut from the base metal and the weld metals to welded single edge notch bending (SENB) specimens. All the cracks were within the weld metal, so the properties of the heat affected zone were not taken into account. It is concluded that the GTN model enabled the crack initiation prediction, and also that the constraint effect originating from different joint width is successfully assessed. The difference in the predicted value of the fracture mechanics parameter, J integral, during blunting and at the beginning of the stable crack growth is shown in Figure 5, for the overmatched and undermatched weld metal with the same joint width.

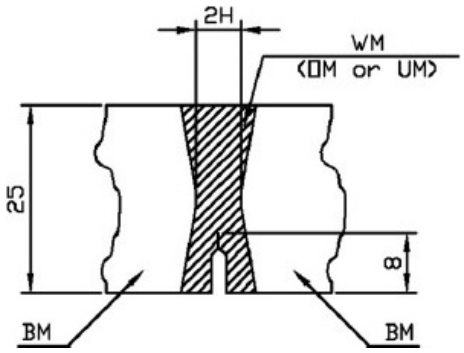

FIGURE 4. Scheme of the welded joint, [**56**].

A detailed description of different zones in a dissimilar welded joint is applied by Yang [**57**]. In this work, an additional heterogeneity of the welded joint exists as a result of different base metals – ferritic steel is joined with austenitic stainless one; this procedure includes the application of 'buttering' alloy on the ferritic side. Two different crack positions were considered, in the very narrow fusion zone and in the heat affected zone. Both of them are on the ferritic side of the joint and are very close to the interfaces between the weld zones. The authors have applied the GTN model, including the procedure proposed by Dutta et al. [**58**], where the value of the constitutive parameter q_2 is taken as variable along the crack path. Also, the part of the joint around the fusion zone is split into several regions with different mechanical properties. A good description of fracture behaviour is obtained for both positions of the initial crack tip.

In [**59**], the GTN model is applied in the analysis of interface regions in dissimilar (ferrite-austenite) steel welded joints, like in [**57**]. One of the main concerns

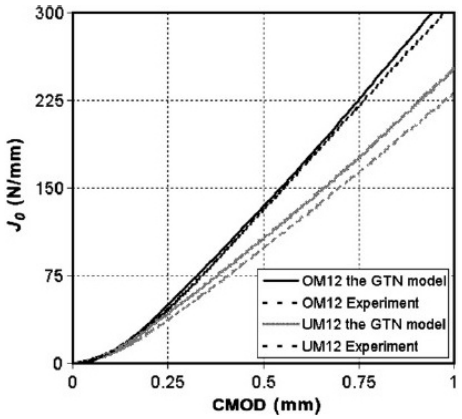

FIGURE 5. Dependence of J integral on CMOD (pre-crack blunting and beginning of stable growth) – OM and UM joints, width 12 mm, [**56**].

was determination of the influence of the local constraint in the vicinity of the crack tip on the fracture resistance. The cracks were positioned on both the ferrite and austenite side of the joint, and the distance between the interfaces and the crack is varied. Four materials were considered (ferrite and austenite BM, weld metal and buttering between the ferrite BM and weld metal), without further subdivision of the joint zones; similar procedure is also applied in an earlier study [**60**]. Authors of [**59**] continued their work on fracture analysis of dissimilar joints by application of the GTN model in [**61**]. A very detailed subdivision of the joint is performed in the numerical model in this work, with 10 subzones; seven of them represent the heat affected zone. Also, many different crack positions are considered, 25 in total. Some of the cracks had significant path deviations, depending on the position and the neighbouring material regions. The authors concluded that the local heterogeneity can cause significant variations in fracture resistance of the joint zones. For existing joints, they propose taking the local heterogeneity into account in fracture mechanics examinations. As for the design of the new joints, the reduction of heterogeneity (obtained by control of the welding process and post-welding treatment) may be beneficial to the fracture toughness of the joint, [**61**].

Negre et al. [**62**] applied the GTN model in the analysis of ductile fracture of laser welded joints (the base metal was Al 6000 alloy). The applied micromechanical model was GTN, and the initial crack was positioned at the interface between the fusion zone and HAZ in CT specimen (for simplicity, base metal was used instead of HAZ in the models, [**62**]). The initial porosity was set equal to the volume fraction of inclusions. Besides the micromechanical model, the authors also applied the cohesive zone modelling technique. The crack growth process was modelled successfully, including the deviation of the crack path obtained by using the GTN model, Figure 6. Cohesive zone modelling was performed on 2D models, while micromechanical modelling was applied on 3D models, which enabled a detailed

insight into stress fields and crack front spatial shape (difference between the surface and interior of the specimen). The same authors also considered two other positions of the cracks in laser welded Al alloy joints in another paper [**63**] – in the base metal and in the fusion zone.

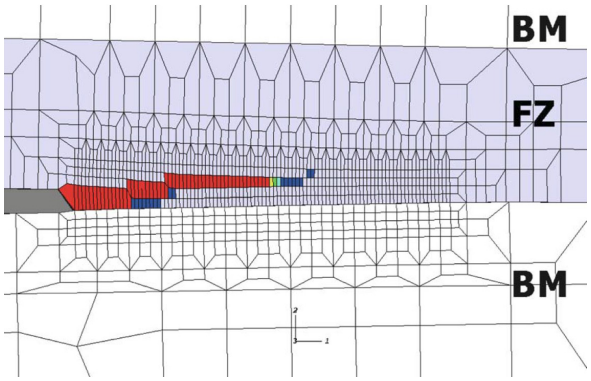

FIGURE 6. Crack path deviation, [**62**].

The work [**64**] presents another example of analysis of damage development in welded aluminium alloys – friction stir welded joints of 2024 alloy are considered. Both 2D and 3D models of the tensile specimen without a pre-crack are applied, and the GTN model is used for damage development prediction. It is shown that variation of the yield stress profile along the joint zone can change the position of the final fracture. Another interesting aspect is considered – distribution of the second-phase void nucleating particles (in the GTN model, their void volume fraction is denoted as f_N, Equation (2.4)). A further advance in modelling is presented in [**65**] (Nielsen et al.) on the example of aluminium alloy 6005, where modification of the GTN model is applied in order to take into account the change of the shape of the voids during the fracture process.

One of the most recent studies dealing with ductile fracture modelling of welded joints is presented by Qiang and Wang [**66**]. The authors used the GTN model in fracture analysis of X80 steel, and the parameters were obtained by analysis of chemical composition and calibration on tensile smooth specimens. The initial crack was positioned in either weld metal, base metal or coarse-grained/fine-grained/intercritical heat affected zone. Having in mind the application of the analysed material (a pipeline steel), single edge notch tension (SENT) specimens were tested in addition to single edge notch bending (SENB). It was previously shown in the literature, e.g. [**67**], that this geometry is better suited than SENB for pipelines with circumferential cracks exposed to axial loading. In addition to analysis of ductile crack growth, the authors of [**66**] also considered the influence of the T-stress for different welded joint regions.

Penuelas et al. [**68**] analysed ductile fracture of steel welded joints using the complete Gurson model (CGM) [**37**]. An interesting approach was applied – instead of using one base metal and different weld metals, specimens with the same

(fixed) weld metal properties and different base metals were considered. In addition to variation of the mismatch ratio, the crack length and joint width were also varied. Through experimental and numerical analysis, the authors quantified the constraint effects through the total constraint parameter, which takes into account both the influence of geometry and material mismatching. In addition to ductile fracture, cleavage fracture is considered by Betegon et al. **[69]**, at different temperatures (note: this is the same research group which published the paper **[68]**). The prediction of both mechanisms was performed by micromechanical modelling; it turned out that the cleavage resistance depends on both temperature and joint configuration, while the resistance to ductile fracture is almost temperature independent.

In **[70]**, fracture analysis of welded joints with one or two weld metals by application of the CGM is presented by the authors of the current work. The joints were undermatched, overmatched, or fabricated with both weld metals, and the base metal was high-strength steel (NIOMOL 490). When stable crack growth is considered, the influence of the overmatched joint width can be seen in Figure 7 (part of the mesh around the crack tip in the SENB specimen is shown). The increase in width decreases the fracture resistance, which is in agreement with the results shown in Figure 9 for crack initiation. The opposite trend, increase in fracture resistance with the increase in joint width, is observed in UM joints, which can be seen in Figure 8. The behaviour of UM and OM joints with respect to their width corresponds to that obtained by Rakin et al. **[56]** by application of the GTN model to these joints, as well as in **[55]**.

The influence of the finite element size on crack growth initiation prediction is shown in Figure 9a, for three OM joint widths. Crack tip opening displacement at crack growth initiation (CTOD_i) is used as fracture parameter, determined by using σ_5 concept **[71]**. The increase in the element size results in prediction of higher resistance to fracture initiation. However, the quantity which influences the prediction of fracture initiation is not the element size itself, but the distance between the integration points within an element. This is also in accordance with the conclusions obtained on macroscopically homogeneous materials in **[72, 73]**. In Figure 9b, the finite elements with dimensions $0.3 \times 0.3\,\mathrm{mm}$ and 3×3 integration give very similar prediction as those with dimensions $0.15 \times 0.15\,\mathrm{mm}$ and 2×2 integration. The distance between the integration points in these two elements is rather similar.

Unfortunately, this is no exception and the application of the local approach to fracture is typically related to mesh-dependence, as mentioned in Section 2. However, much more important is the transferability of the FE size – once determined, it is used on other geometries. In this way, the size of the element becomes one of micromechanical parameters, which is transferred to other configurations along with the other parameters (such as f_0, etc.).

In **[70]**, the authors also gave the example with two different weld metals and a crack which grows through both of them. One of the weld metals is overmatched, while the other one is undermatched, which represents additional heterogeneity within the weld itself. The micromechanical parameters were transferred from the

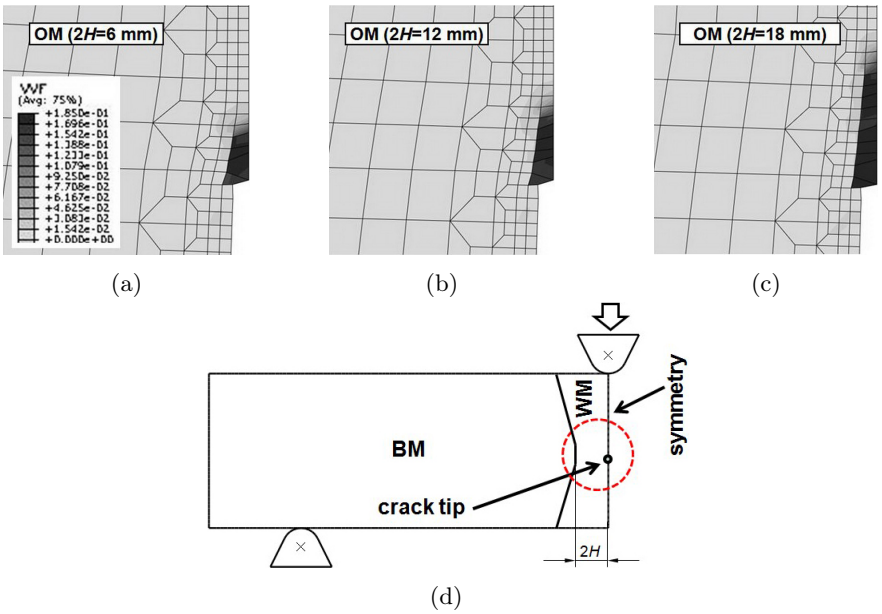

FIGURE 7. Crack growth for OM joint with width: 6 mm (a), 12 mm (b) and 18 mm (c) [70] and scheme of the welded specimen; symmetry is applied in modelling (d).

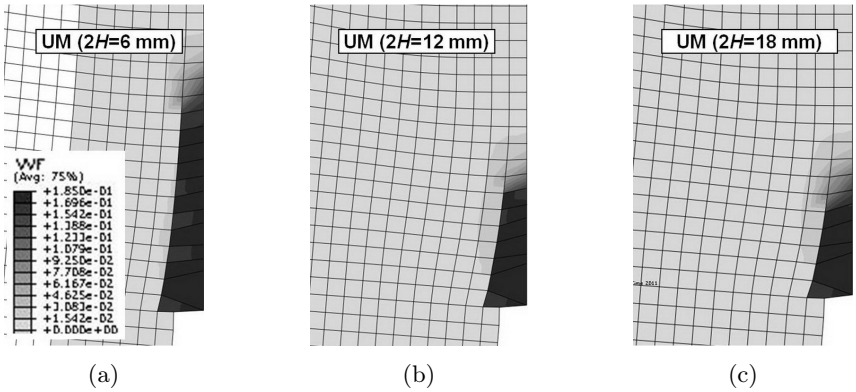

FIGURE 8. Crack growth for UM joint with width: 6 mm (a), 12 mm (b) and 18 mm (c) [**70**].

configurations with a single weld metal, and more significant crack growth in the overmatched weld metal is predicted successfully, Figure 10.

In the study [**74**], two different configurations of the cracks in steel weldments are considered by using the CGM: a surface crack in a tensile panel (TP) and an edge crack in a standard SENB specimen exposed to bending. Two positions of the

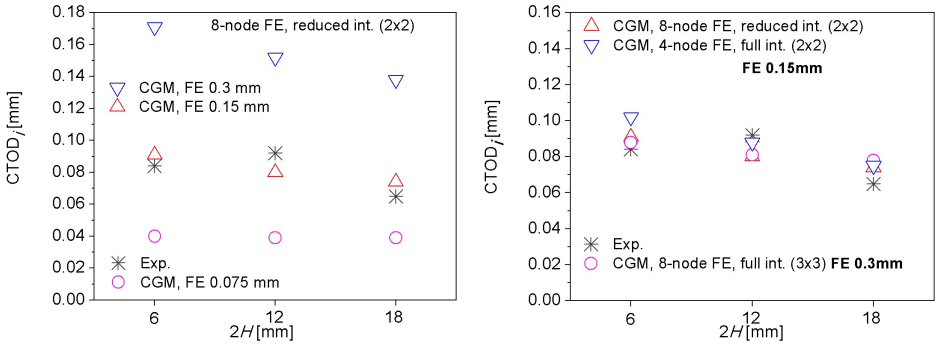

(a) (b)

FIGURE 9. Influence of the size and integration order on resistance to fracture initiation [**70**].

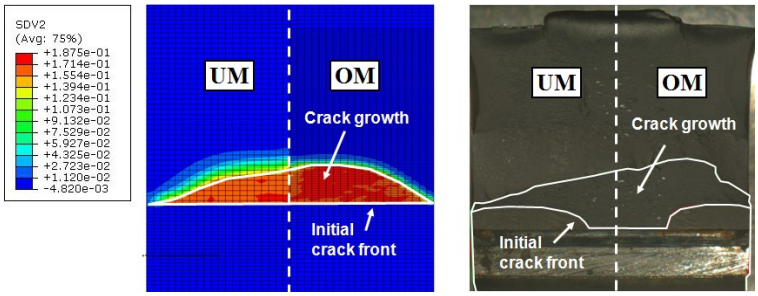

FIGURE 10. Crack growth in the joint with two weld metals and a crack through both of them – fracture surface of SENB specimen [**70**].

cracks were analysed in each geometry: in the weld metal and in the heat affected zone. The models of the specimens with a pre-crack in HAZ are shown in Figure 11.

In Figure 12, the J integral values at the moment of crack initiation, J_i, determined experimentally and predicted through application of the micromechanical model, are shown. The same values of micromechanical parameters are applied in both geometries (transferred), and the effects of heterogeneity of the joint and different constraint conditions (caused by the pre-crack shape and loading mode) are captured successfully by micromechanical modelling. An interesting aspect of this study is the method for characterisation of the joint zones: WM, BM, coarse grain HAZ and fine grain HAZ – their properties were determined by a single-specimen procedure, Younise et al. [**75**]. This procedure includes application of digital image correlation (measurement of tensile strains using the Gom Aramis stereometric system) and numerical analysis of tensile testing of a welded plate specimen.

Song at al. [**76**] considered another aspect which may influence the ductile fracture behaviour of welded joints: the pre-strain history, introduced through the

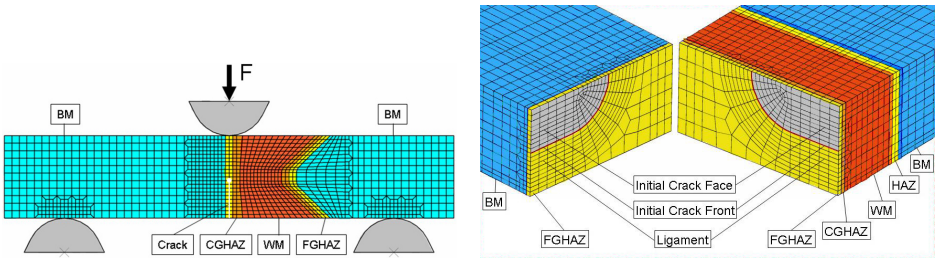

(a) (b)

FIGURE 11. FE meshes – SENB specimen (a) and tensile panel TP (b) – initial cracks in HAZ [**74**].

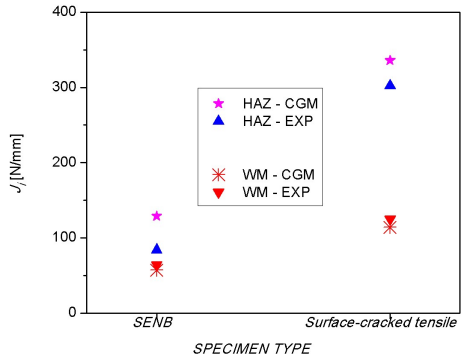

FIGURE 12. J integral at crack initiation for SENB and tensile panel TP – initial cracks in WM or HAZ [**74**].

pre-strain cycles. The pre-strain cycles were either symmetrical or non-symmetrical, and the relation between these cycles and mismatch effect (the joints were over-matched) was analysed by application of the CGM on welded SENT specimens. The authors concluded that the pre-straining influenced the fracture resistance of the analysed joints. Also, it turned out that the initial crack length did not affect their fracture resistance significantly.

Nielsen and Tvergaard [**77**] have dealt with the influence of the shear failure – a failure mode which cannot be simulated by the Gurson model, GTN or CGM in their original forms. Therefore, some studies have been devoted to extending the GTN model to such loading and failure development mode, e.g. by Nahshon and Hutchinson [**46**], or Xue [**47**], as mentioned in Section 2.2. The former is applied, and also modified, in the analysis of spot-welded joints in [**77**], Figure 13. It should be noted that the damage parameter, void volume fraction, in Equation (2.3) has one more component to take shearing into account, denoted by the authors as $f_{\text{modification}}$. It is concluded that the benefit from application of the shear modification of the model is pronounced for small diameters of the spot weld. Also, the

influence of the shearing mode is found in the welds with a larger diameter, where it especially affected the prediction of fracture initiation. Nielsen [**78**] compared different modifications of three micromechanical models: GTN, shear-modified GTN by Nahshon and Hutchinson and the model of Gologanu, Leblond and Devaux (the second and the third one take into account the effects of shear loading in ductile fracture analysis). All of them are applied to spot welded joints exposed to either tensile or shear loading.

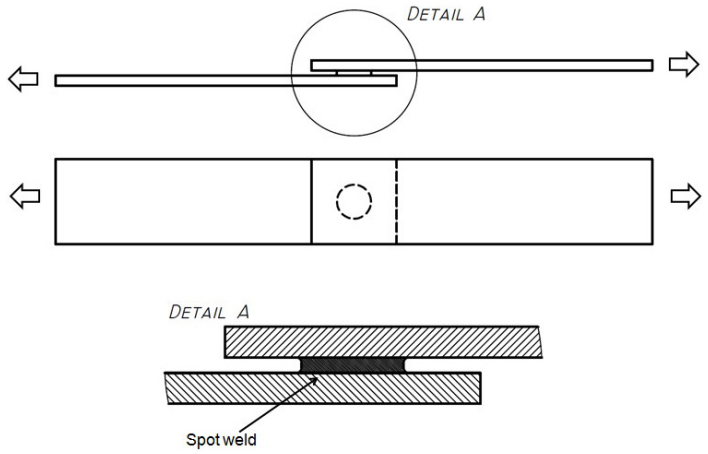

FIGURE 13. Scheme of the specimen with spot weld.

4. Application of micromechanical models in fracture analysis of welded structures

This section presents some studies and results obtained on welded structures or non-standard welded specimens. Having in mind the need for determination of tensile properties and micromechanical parameters of the materials (joint zones), most of them also include the testing of standard specimens for mechanical characterisation and/or standard fracture mechanics specimens, such as CT or SENB.

The GTN micromechanical model is applied in [**79**] to predict ductile fracture resistance of laser-hybrid steel joints. The micromechanical parameters are obtained by a combination of metallographic analysis, fitting procedure and unit cell analysis. A special attention is given to the deviation of the crack path obtained for the cracks located in the vicinity of the fusion line on welded CT specimens. After a detailed micromechanical analysis of welded specimens, the same set of parameters is applied on a beam-column connection with a semi-eliptical pre-crack in the welded joint. It is obtained that fracture initiation resistance is higher for the structure with the surface crack than in the standard specimen; this is in agreement with the results from [**74**], Figure 12, and can be attributed to different constraint conditions caused by the crack shape.

Chhibber et al. [**80**] applied the GTN model in a similar examination procedure, where the results were first obtained on the welded and base metal (SA333 Gr.6 Carbon Steel) specimens. They performed a parametric study, aimed at determination of the micromechanical parameters without metallographic analysis. Five parameters were varied (f_0, f_c, f_f, ε_N, f_N), while the remaining ones were kept constant. Finally, the values of the parameters were applied in the fracture analysis of a pre-cracked pipe produced from the mentioned material; the prediction was successful, based on the comparison of force-load line displacement curve and crack growth resistance curve. Also, the authors commented on the inter-dependence of the parameters, which points out the fact that multiple parameter sets can give good fracture description (non-uniqueness). A similar conclusion can also be found in some previous studies on macroscopically homogeneous materials.

Two recent articles present the application of the local approach to fracture to welded components – [**81**] (pipe with a weld defect) and [**82**] (connection between a column and flange). The examination in [**81**] includes the standard tensile specimens, notched specimens and single-edge tensile specimens for determining the properties of the joint zones. The GTN model parameters are transferred to a welded pipeline segment produced from X65 steel (length of the segment was 6 m). The combined effect of the internal pressure and bending load is analysed, as well as significance of the boundary conditions. The authors conclude that the applied local approach-based methodology "can be useful for a fine analysis of tests but is clearly not mature enough to be used as a routine failure assessment procedure".

In the study [**82**], a different geometry is analysed in comparison with [**80**] and [**81**] – a welded connection between the load-carrying members, Figure 14. The uncoupled approach to fracture is applied, based on the modified Rice–Tracey model – Stress Modified Critical Strain (SMCS), Section 2. The model is applied through a user subroutine in Abaqus, which enables not only tracking the fracture initiation, but also crack growth through the welded joint. The authors conclude that the applied fracture criteria can predict ductile fracture behaviour of the analysed welded connections. However, the model predicts lower displacement values until final failure. When comparing the stage of significant crack growth, the Rice-Tracey model gave better results than SMCS; an example is shown in Figure 14 – the Rice–Tracey model is referred to as VGM or void growth model.

The Stress Modified Critical Strain model is also applied by Kanvinde et al. in [**83**], along with the classical approach of elastic-plastic fracture mechanics based on J integral. The authors mention that the study is one of the first applications of this model to structural fillet welds. Fracture behaviour of cruciform welded joints with sharp root notches, produced from the base material A572 steel (Grade 345), is analysed. The length of the root notch, filler material and the dimensions of the joint are varied; 24 combinations in total. Fracture surface examination revealed that all the tested welds finally failed by brittle fracture, but ductile crack growth was present in the initial stage. The authors report that the "SMCS model can predict fracture in the structural fillet welds with good accuracy, while the J integral based methods result in somewhat conservative and inaccurate predictions of fracture", [**83**]. Such a conclusion is mainly based on the ability of the two

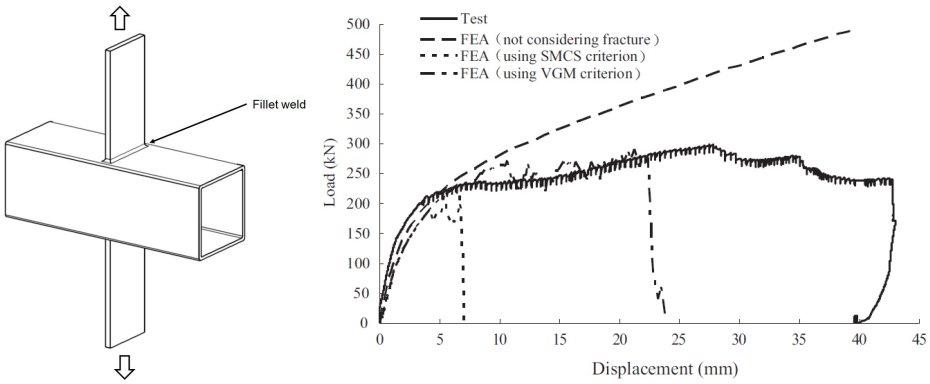

(a) (b)

FIGURE 14. Scheme of the joint analysed in [**82**] (a) and load-displacement curves, [**82**] (b).

approaches to predict the weld deformation at fracture. Regarding the SMCS model, acceptable transferability of parameters between different welded geometries has been achieved, even though some aspects, such as local property variations, were not taken into account.

In a recent paper [**84**], the authors applied the SMCS model and the Rice–Tracey model, in the analysis of welded steel hollow spherical joints (a characteristic geometry, typically applied to space grid structures). Behaviour of the spherical joints was analysed under axial tensile loading, and also under compressive loading. Fracture was dominant failure mechanism under tension, while loss of stability of the sphere was critical under compressive loading. Finally, the authors proposed a simplified SMCS or S-SMCS model, stating that it is more convenient for practical application to the examined joints. This is done by setting the triaxiality ratio to a constant value, thus obtaining the failure criterion which depends only on the plastic strain.

An interesting analysis is shown in [**85**], where both static and dynamic loading of the welded connections are considered. Namely, the authors applied a modification of the GTN model which takes into account both isotropic and kinematic hardening. Therefore, micromechanical analysis was successfully applied in assessment of ductile fracture under static, but also dynamic loading conditions (ultra low cycle fatigue).

Ma et al. [**86**] proposed a modification of the Xue model [**87**] based on damage plasticity, which takes into account shear loading, and applied it to the tubular connections, Figure 15. The authors propose a simplified calibration procedure for the model, aimed at more convenient engineering usage. It is worth mentioning that this simplification is motivated by the Rice-Tracey approach [**24**], which once again proves its importance and applicability almost 50 years after publication. The authors state that they successfully predicted the sequence of failure, which is observed in the welded connection during the experiments, [**86**].

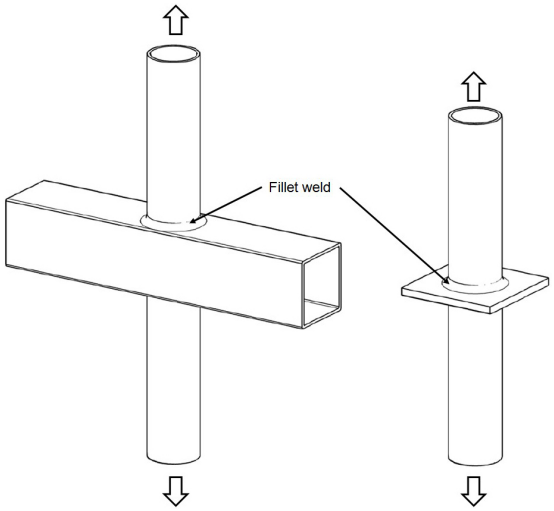

FIGURE 15. Schematic view of non-rigid and rigid joints analysed in [**86**].

In a recent article, Liu et al. [**88**] considered the fracture of tubular welded joints (similar configuration as the one shown in Figure 15, left-hand side) using a modification of the GTN model which takes into account void shearing. This modification is performed through addition of another scalar variable: shear stress-related damage. In this way, the evolution of porosity is tracked by the GTN model, while the shearing is taken into account through the mentioned additional damage variable. The modified model gave better results in the case of shear-dominated stress fields. To be more precise, the fracture initiation is successfully predicted by the GTN model, but the advantage of the modified model is primarily in the simulation of the crack growth process, where shear stress state is much more pronounced in the analysed geometry.

Prediction of fracture initiation on the structures without an initial crack is presented by Medjo et al. in [**89**], on the example of structures with a blunt stress concentrator–machined notch. The models of casing seam pipes (produced from steel API J55) with notches are considered. The shape of the notch is either circular, or elongated in axial direction, Figure 16a. The influence of the weld is not analysed, since the volumetric defects are considered. It is obtained that the prediction of fracture initiation in this case does not depend on the mesh size; CGM is applied. In [**89**], it is also shown that the integration order does not have an influence on the crack initiation in these geometries. A similar conclusion related to the mesh dependence on blunt stress concentrators is obtained in [**51**], mentioned in the previous section – flat welded tensile specimens with U-notches are reported to exhibit very slight mesh dependence. The U-notches analysed in [**51**] had radius 2 mm, so they were more pronounced stress concentrators in comparison with the pipes from Figure 16.

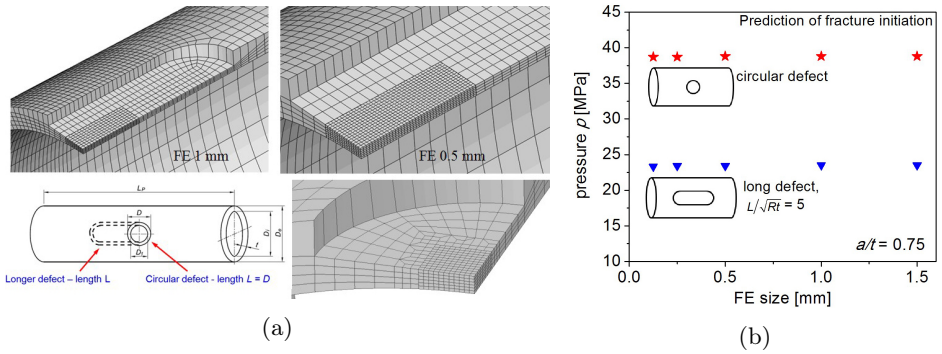

(a) (b)

FIGURE 16. Pipe with blunt defect (a) and pressure corresponding to fracture initiation – influence of defect length and FE size; based on **[89]** (b).

Now, we will show a comparison of the stress conditions in one of the pipe geometries from Figure 16a with the conditions in cylindrical specimens. A circular notch on the pipe, with depth equal to 75 % of the wall thickness, is considered. Such depth indicates that the pipe is significantly weakened by this machined defect. Round tensile (RT) and two notched tensile specimens are used for comparison; notch radius is either 10 mm (NT10) or 2 mm (NT2), Figure 17a. The positions for

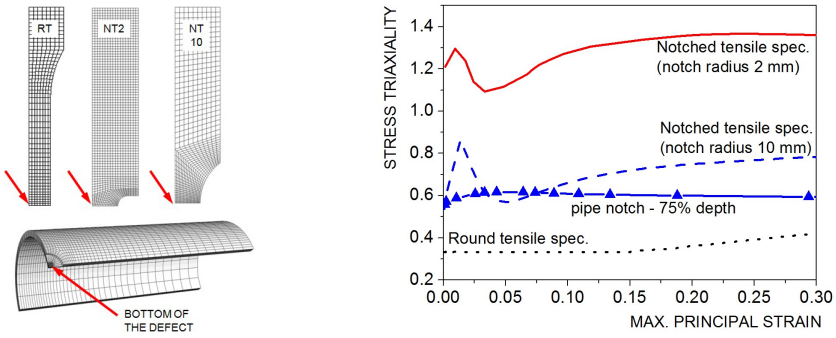

(a) (b)

FIGURE 17. Finite element meshes – cylindrical specimens and a notched pipe (a) and dependence of stress triaxiality on strain (b).

tracking the stress triaxiality values are marked by the arrows. Triaxiality at the bottom of the pipe notch is generally in the range between NT10 and RT specimen, hence it can be said that the stress concentration is weakly pronounced, Figure 17b.

Application of the CGM on the example of a welded structure – thin-walled seam pipe, is shown in **[90]** by the authors of this paper. Actually, fracture assessment is performed on the non-standard pipe ring notched specimens, proposed

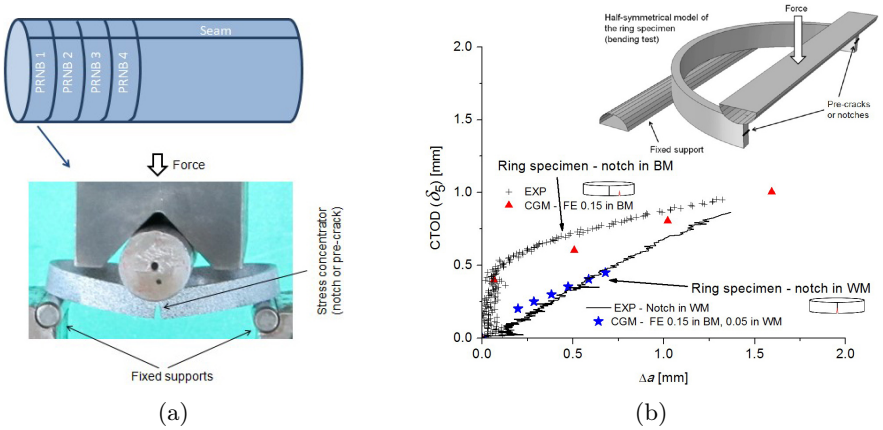

FIGURE 18. Cutting scheme of the ring specimens and testing setup (a) and fracture resistance curves – seam and BM; based on **[90]** (b).

as testing geometry for characterisation of the pipeline materials, **[91–93]**. The scheme which shows the preparation of the specimens is shown in Figure 18a; the pipe is fabricated by welding, i.e. it is a seam pipe. One of the aims was to determine the difference in fracture behaviour of the base metal and the seam, therefore the stress concentrators were fabricated in both the base metal and the seam. The fracture resistance of the weld metal turned out to be lower in comparison with the base metal, Figure 18b. Seamless pipes were also considered in **[90]**, and they generally showed better fracture resistance in comparison with the seam ones for the considered material (pressure vessel steel) and dimensions.

5. Concluding remarks

Problems of fracture of welded joints are an important topic in integrity assessment of welded structures in different industries. In this work, application of micromechanical models in fracture analysis of welded joints is given from a group of studies, including a number of papers published by the authors of this work. A brief overview of the models is presented at the beginning.

From the studies listed in this work, it can be concluded that the micromechanical models of the local approach to ductile fracture can be used to predict the fracture behaviour of both homogeneous and inhomogeneous materials, provided that proper determination of material properties and model parameters has been performed. Many recent studies which use some of these models and corresponding failure criteria can be regarded as a proof of this conclusion. A very wide range of problems has been successfully treated by application of the local approach, from detailed analyses of phenomena in the material during fracture to macroscopic behaviour of structures with cracks. In this work, only the studies which deal with welded joints are presented, while many articles which deal with macroscopically

homogeneous materials can also be found in the literature. It is worth mentioning that some of the presented studies also contain proposals for modifications of the existing micromechanical models. This represents their contribution to the development of the local approach in general, motivated by the complexity of the problems of welded joints fracture.

Generally, one of the most important advantages of the local approach to fracture, in comparison with the so-called global approach of fracture mechanics, is the transferability of the model parameters between different geometries. Also, the ability of micromechanical models to successfully 'capture' the heterogeneity of the material properties and its effect on fracture is especially beneficial for the analysis of welded joints. Unlike global fracture mechanics, the local approach can be applied to structures without initial cracks. However, a significant drawback of the micromechanical models for ductile fracture analysis is mesh dependence (except for fracture initiation on blunt stress concentrators), which is typically resolved by treatment of the finite element size as a material parameter in the model.

Acknowledgments. This work was supported by the Ministry of Education, Science and Technological Development of the Republic of Serbia (Contracts No. 451-03-68/2020-14/200135, 451-03-68/2020-14/200105).

References

1. O. Blodgett, *Design of Welded Structures*, James F. Lincoln Arc Welding Foundation, 1966.
2. K. Masubuchi, *Analysis of Welded Structures*, Elsevier, 1980.
3. L. Liu, *Welding and Joining of Magnesium Alloys*, Woodhead Publishing, 2010.
4. Q. Sun, J. Li, Y. Liu, J. Feng, *Narrow gap welding for thick titanium plates: a review*, in: S. Chen, Y. Zhang, Z. Feng (eds.), *Transactions on Intelligent Welding Manufacturing*, Springer, Singapore, 2019, 29–54.
5. D. Grewell, A. Benatar, *Welding of plastics: fundamentals and new developments*, Int. Polym. Proc. **22** (2007), 43–60.
6. S. A. Vendan, M. Natesh, A. Garg, L. Gao, *Polymer welding techniques and its evolution*, chapter in: *Confluence of Multidisciplinary Sciences for Polymer Joining*, Springer, Singapore, 2019, 11–71.
7. A. Pineau, A. Benzerga, T. Pardoen, *Failure of metals I: Brittle and ductile fracture: overview article*, Acta Mater. **107** (2016), 424–483.
8. E. M. Hackett, K. H. Schwalbe, R. H. Dodds Jr. (eds.), *Constraint Effects in Fracture*, ASTM STP **1171**, ASTM, Philadelphia, 1993.
9. G. Pluvinage, J. Capelle, M. Hadj Méliani, *A review of the influence of constraint on fracture toughness*, Struct. Integr. Life **14** (2014), 65–78.
10. *BS 7910 Guide to methods for assessing the acceptability of flaws in metallic structures*, British Standards Institution (BSI), London, 2015.
11. K. H. Schwalbe, M. Koçak (eds.), *Mismatching of Interfaces and Welds*, GKSS Research Center Publications, Geesthacht, 1997.
12. K. H. Schwalbe, R. A. Ainsworth, C. Eripret, C. Franco, P. Gilles, M. Koçak, et al., *Common views on the effects of yield strength mis-match on testing and structural assessment*, in: K. H. Schwalbe, M. Koçak (eds.), *Mis-matching of Interfaces and Welds*, GKSS Research Center, Geesthacht, 1997, 99–132.
13. K. H. Schwalbe, Y. J. Kim, S. Hao, A. Cornec, M. Kocak, *EFAM ETM-MM 96 - the ETM method for assessing the significance of crack-like defects in joints with mechanical heterogeneity* (*strength mismatch*), GKSS Research Center, Geesthacht, 1997.

14. M. C. Burstow, I. C. Howard, *Damage mechanics models of ductile crack growth in welded specimens*, Fatigue Fract. Eng. Mat. Struct. **23** (2000), 691–708.
15. C. Betegon, I. Penuelas, *A constraint based parameter for quantifying the crack tip stress fields in welded joints*, Eng. Fract. Mech. **73** (2006), 1865–1877.
16. M. Toyoda, *Transferability of fracture mechanics parameters to fracture performance evaluation of welds with mismatching*, Prog. Struct. Eng. Mater. **4** (2002), 117–125.
17. U. Zerbst, R. A. Ainsworth, H. Th. Beier, H. Pisarski, Z. L. Zhang, K. Nikbin, T. Nitschke-Pagel, S. Münstermann, P. Kucharczyk, D. Klingbeil, *Review on fracture and crack propagation in weldments - A fracture mechanics perspective*, Eng. Fract. Mech. **132** (2014), 200–276.
18. U. Zerbst, *Application of fracture mechanics to welds with crack origin at the weld toe: a review Part 1: Consequences of inhomogeneous microstructure for materials testing and failure assessment*, Weld. World **63** (2019), 1715–1732.
19. U. Zerbst, *Application of fracture mechanics to welds with crack origin at the weld toe—a review. Part 2: Welding residual stresses. Residual and total life assessment*, Weld. World (2019) https://doi.org/10.1007/s40194-019-00816-y.
20. P. Kucharczyk, M. Madia, U. Zerbst, B. Schork, P. Gerwien, S. Münstermann, *Fracture-mechanics based prediction of the fatigue strength of weldments. Material aspects*, Eng. Fract. Mech. **198** (2018), 79–102.
21. J. Besson, *Continuum models of ductile fracture: a review*, Int. J. Damage Mech. **19** (2010), 3–52.
22. A. Benzerga, J. Leblond, A. Needleman, V. Tvergaard, *Ductile failure modelling*, Int. J. Fract. **201** (2016), 29–80.
23. A. Pineau, *Development of the local approach to fracture over the past 25 years: theory and applications*, Int. J. Fract. **138** (2006), 139–166.
24. J. R. Rice, D. M. Tracey, *On the ductile enlargement of voids in triaxial stress fields*, J. Mech. Phys. Solids **17** (1969), 201–217.
25. F. M. Beremin, *Experimental and numerical study of the different stages in ductile rupture: application to crack initiation and stable crack growth*, in: S.Nemat-Nasser (ed.), *Three-dimensional Constitutive Relations and Ductile Fracture*, North-Holland Publications, Amsterdam, 1981, 185–205.
26. J. W. Hancock, A. C. Mackenzie, *On the mechanics of ductile failure in high-strength steel subjected to multi-axial stress-states*, J. Mech. Phys. Solids **24** (1976), 147–169.
27. Y. Huang, *Accurate dilatation rates for spherical voids in triaxial stress fields*, Trans. ASME: J. Appl. Mech. **58** (1991), 1084–1086.
28. N. L. Dung, *A simple model for the three-dimensional growth of voids/inclusions in plastic materials*, Int. J. Fract. **53** (1992), R19–R25.
29. C. Chaouadi, P. de Meester, W. Vandermeulen, *Damage work as ductile fracture criterion*, Int. J. Fract. **66** (1994), 155–164.
30. T. J. Wang, *A new ductile fracture theory and its applications*, Acta Mech. Sinica **11** (1995), 83–93.
31. B. K. Dutta, H. S. Kushwaha, *A modified damage potential to predict crack initiation: theory and experimental verification*, Eng. Fract. Mech. **71** (2004), 263–275.
32. G. Rousselier, *Ductile fracture models and their potential in local approach of fracture*, Nucl. Eng. Design **105** (1987), 97–111.
33. A. L. Gurson, *Continuum theory of ductile rupture by void nucleation and growth: part I - yield criteria and flow rules for porous ductile media*, J. Eng. Mater. Technol. - Trans. ASME **99** (1977), 2–15.
34. V. Tvergaard, *Influence of voids on shear band instabilities under plane strain conditions*, Int. J. Fract. **17** (1981), 389–407.
35. V. Tvergaard, A. Needleman, *Analysis of cup–cone fracture in a round tensile bar*, Acta Metall. **32** (1984), 157–169.
36. C Chu, A Needleman, *Void nucleation effects in biaxiality stretched sheets*, ASME, J. Eng. Mater. Technol. **102** (1980), 249–256.

37. Z. L. Zhang, C. Thaulow, J. Odegard, *A complete Gurson model approach for ductile fracture*, Eng. Fract. Mech. **67** (2000), 155–168.
38. T. Pardoen, J. Besson, *Micromechanics-based constitutive models of ductile fracture*, in: Clotilde Berdin et al. (eds.), *Local Approach to Fracture*, Presses de l'Ecole des Mines, Paris, 2004, 221–264.
39. Z. L. Zhang, *A complete Gurson model*, in: M. H. Aliabadi (ed.), *Nonlinear Fracture and Damage Mechanics*, WIT Press, Southampton, 2001, 223–248.
40. P. F. Thomason, *Ductile Fracture of Metals*, Pergamon Press, Oxford, 1990.
41. T. Pardoen, J. W. Hutchinson, *An extended model for void growth and coalescence*, J. Mech. Phys. Solids **48** (2000), 2467–2512.
42. Z. L. Zhang, *A Practical Micro-Mechanical Model-Based Local Approach Methodology for the Analysis of Ductile Fracture of Welded T-Joints*, Ph.D. thesis, Lappeenranta University Of Technology, Finland, 1994.
43. B. Tanguy, T. T. Luu, G. Perrin, A. Pineau, J. Besson, *Plastic and damage behavior of a high strength X100 pipeline steel: experiments and modelling*, Int. J. Pres. Ves. Pip. **85** (2008), 322–335.
44. M. Gologanu, J. B. Leblond, J. Devaux, *Approximate models for ductile metals containing non–spherical voids-case of axisymmetric prolate ellipsoidal cavities*, J. Mech. Phys. Solids **41** (1993), 1723–1754.
45. M. Gologanu, J. B. Leblond, J. Devaux, *Approximate models for ductile metals containing non-spherical voids - case of axisymmetric oblate ellipsoidal cavities*, J. Eng. Mater. Technol. **116** (1994), 290–297.
46. K. Nahshon, J. W. Hutchinson, *Modification of the Gurson Model for shear failure*, Eur. J. Mech. A-Solids **27** (2008), 1–17.
47. L. Xue, *Constitutive modeling of void shearing effect in ductile fracture of porous materials*, Eng. Fract. Mech. **75** (2008), 3343–3366.
48. Y. W. Shi, *Critical void growth for ductile rupture of steel welds*, Eng. Fract. Mech. **34** (1989), 901–907.
49. A. Al Rassis, A. Imad, M. Nait Abdelaziz, G. Mesmacque, A. Amrouche, C. Eripret, *A numerical study of the ductile tearing in welded joints using the Rice–Tracey void growth model*, J. Phys. IV **06** (1996), C6-13–C6-21.
50. J. Wilsius, A. Imad, M. Nait Abdelaziz, G. Mesmacque, C. Eripret, *Void growth and damage models for predicting ductile fracture in welds*, Fatigue Fract. Eng. Mat. Struct. **23** (2006), 105–112.
51. L. Kang, H. Ge, T. Kato, *Experimental and ductile fracture model study of single-groove welded joints under monotonic loading*, Eng. Struct. **85** (2015), 36–51.
52. H. Y. Tu, S. Schmauder, U. Weber, *Simulation of the fracture behavior of Al6061 laser welded joints with the Rousselier model*, Comp. Mater. Sci. **116** (2016), 122–128.
53. H. Y. Tu, S. Schmauder, U. Weber, Y. Rudnik, V. Ploshikhin, *Simulation of the damage behaviour of electron beam welded joints with the Rousselier model*, Eng. Fract. Mech. **103** (2013), 153–161.
54. G. Lin, Y. J. Kim, A. Cornec, K. H. Schwalbe, *Numerical analysis of ductile failure of under-matched interleaf in tension*, Int. J. Fract. **91** (1998), 323–347.
55. X. Y. Li, Q. Hao, Y. W. Shi, Y. P. Lei, G. Marquis, *Influence of mechanical mismatching on the failure of welded joints by void nucleation and coalescence*, Int. J. Pres. Ves. Pip. **80** (2003), 647–654.
56. M. Rakin, N. Gubeljak, M. Dobrojević, A. Sedmak, *Modelling of ductile fracture initiation in strength mismatched welded joint*, Eng. Fract. Mech. **75** (2008), 3499–3510.
57. J. Yang, *Micromechanical analysis of in-plane constraint effect on local fracture behavior of cracks in the weakest locations of dissimilar metal welded joint*, Acta Metall. Sin. (Engl. Lett.) **30** (2017), 840–850.
58. B. K. Dutta, S. Guin, M. K. Sahu, M. K. Samal, *A phenomenological form of the q_2 parameter in the Gurson model*, Int. J. Pres. Ves. Pip. **85** (2008), 199–210.

59. K. Fan, G. Z. Wang, F. Z. Xuan, S. T. Tu, *Local fracture resistance behavior of interface regions in a dissimilar metal welded joint*, Eng. Fract. Mech. **136** (2015), 279–291.
60. M. K. Samal, K. Balani, M. Seidenfuss, E. Roos, *An experimental and numerical investigation of fracture resistance behaviour of a dissimilar metal welded joint*, Proc. IMechE Part C: J. Mech. Eng. Sci. **223** (2009), 1507–1523.
61. K. Fan, G. Z.Wang, F. Z. Xuan, S. T. Tu, *Local failure behavior of a dissimilar metal interface region with mechanical heterogeneity*, Eng. Fail. Anal. **59** (2016), 419–433.
62. P. Nègre, D. Steglich, W. Brocks, *Crack Extension at an Interface, Prediction of fracture toughness and simulation of crack path deviation*, Int. J. Fract. **134** (2005), 209–229.
63. P. Nègre, D. Steglich, W. Brocks, *Crack extension in aluminium welds: a numerical approach using the Gurson–Tvergaard–Needleman model*, Eng. Fract. Mech. **71** (2004), 2365–2383.
64. K. L. Nielsen, *Ductile damage development in friction stir welded aluminum (AA2024) joints*, Eng. Fract. Mech. **75** (2008), 2795–2811.
65. K. L. Nielsen, T. Pardoen, V. Tvergaard, B. de Meester, A. Simar, *Modelling of plastic flow localisation and damage development in friction stir welded 6005A aluminium alloy using physics based strain hardening law*, Int. J. Solids Struct. **47** (2010), 2359–2370.
66. B. Qiang, X. Wang, *Ductile crack growth behaviors at different locations of a weld joint for an X80 pipeline steel: A numerical investigation using GTN models*, Eng. Fract. Mech. **213** (2019), 264–279.
67. J. Xu, Z. L. Zhang, E. Østby, B. Nyhus, D. B. Sun, *Constraint effect on the ductile crack growth resistance of circumferentially cracked pipes*, Eng. Fract. Mech. **77** (2010), 671–684.
68. I. Penuelas, C. Betegon, C. Rodriguez, *A ductile failure model applied to the determination of the fracture toughness of welded joints, numerical simulation and experimental validation*, Eng. Fract. Mech. **73** (2006), 2756–2773.
69. C. Betegon, I. Penuelas, J. J. del Coz, *Numerical analysis of the influence of material mismatching in the transition curve of welded joints*, Eng. Fract. Mech. **75** (2008), 3464–3482.
70. M. Rakin, B. Međo, N. Gubeljak, A. Sedmak, *Micromechanical assessment of mismatch effects on fracture of high-strength low alloyed steel welded joints*, Eng. Fract. Mech. **109** (2013), 221–235.
71. *GKSS - Displacement gauge system for applications in fracture mechanics*, Patent publication. GKSS Research Center Publications, Geesthacht, 1991.
72. C. Poussard, C. Sainte Catherine, *A synthesis of numerical round robin on local approach to simulate the brittle to ductile transitions curve by a RPV steel*, in: J. Besson, D. Steglich, D. Moinereau (eds.), *Proceedings of the 9^{th} European Mechanics of Materials Conference EUROMECH - MECAMAT*, Moret-sur-Loing, 2006, 279–284.
73. M. Rakin, Z. Cvijović, V. Grabulov, S. Putić, A. Sedmak, *Prediction of ductile fracture initiation using micromechanical analysis*, Eng. Fract. Mech. **71** (2004), 813–827.
74. B. Younise, M. Rakin, N. Gubeljak, B. Međo, A. Sedmak, *Effect of material heterogeneity and constraint conditions on ductile fracture resistance of welded joint zones - micromechanical assessment*, Eng. Fail. Anal. **82 C** (2017), 435–445.
75. B. Younise, M. Rakin, N. Gubeljak, B. Međo, M. Burzić, M. Zrilić, A. Sedmak, *Micromechanical analysis of mechanical heterogeneity effect on the ductile tearing of weldments*, Mater. Design **37** (2012), 193–201.
76. W. Song, X. Liu, F. Berto, J. Xu, H. Fang, *Numerical simulation of prestrain history effect on ductile crack growth in mismatched welded joints*, Fatigue Fract. Eng. Mater Struct. **40** (2017), 1472–1483.
77. K. L. Nielsen, V. Tvergaard, *Ductile shear failure or plug failure of spot welds modelled by modified Gurson model*, Eng. Fract. Mech. **77** (2010), 1031–1047.
78. K. L. Nielsen, *Predicting failure response of spot welded joints using recent extensions to the Gurson model*, Comp. Mater. Sci. **48** (2010), 71–82.
79. A. Nonn, W. Dahl, W. Bleck, *Numerical modelling of damage behaviour of laser-hybrid welds*, Eng. Fract. Mech. **75** (2008), 3251–3263.

80. R. Chhibber, P. Biswas, N. Arora, S. R. Gupta, B. K. Dutta, *Micromechanical modelling of weldments using GTN model*, Int. J. Fract. **167** (2011), 71–82.
81. C. Soret, Y. Madi, V. Gaffard, J. Besson, *Local approach to fracture applied to the analysis of a full size test on a pipe containing a girth weld defect*, Eng. Fail. Anal. **82** (2017), 404–419.
82. F. Liao, W. Wang, Y. Chen, *Ductile fracture prediction for welded steel connections under monotonic loading based on micromechanical fracture criteria*, Eng. Struct. **94** (2015), 16–28.
83. A. M. Kanvinde, B. V. Fell, I. R. Gomez, M. Roberts, *Predicting fracture in structural fillet welds using traditional and micromechanical fracture models*, Eng. Struct. **30** (2008), 3325–3335.
84. Y. Yin, X. Che, Z. Li, J. Li, Q. Han, *Ductile fracture analysis of welded hollow spherical joints subjecting axial forces with micromechanical fracture models*, Int. J Steel Struct. **19** (2019), 2010–2023.
85. X. Huang, L. Tong, F. Zhou, Y. Chen, *Prediction of fracture behavior of beam-to-column welded joints using micromechanics damage model*, J. Constr. Steel Res. **85** (2013), 60–72.
86. X. Ma, W. Wang, Y. Chen, X. Qian, *Simulation of ductile fracture in welded tubular connections using a simplified damage plasticity model considering the effect of stress triaxiality and Lode angle*, J. Constr. Steel Res. **114** (2015), 217–236.
87. L. Xue, *Stress based fracture envelope for damage plastic solids*, Eng. Fract. Mech. **76** (2009), 419–438.
88. J. Liu, S. Yan, X. Zhao, *Simulation of fracture of a tubular X-joint using a shear-modified Gurson–Tvergaard–Needleman model*, Thin-Walled Struct. **132** (2018), 120–135.
89. B. Medjo, M. Rakin, M. Arsić, Ž. Šarkoćević, M. Zrilić, S. Putić, *Determination of the load carrying capacity of damaged pipes using local approach to fracture*, Mater. Trans. – JIM **53** (2012), 185–190.
90. W. Musrati, B. Medjo, N. Gubeljak, P. Štefane, D. Veljić, A. Sedmak, M. Rakin, *Fracture assessment of seam and seamless steel pipes by application of the ring-shaped bending specimens*, Theor. Appl. Fract. Mech. **103** (2019), paper No. 102302.
91. Y. G. Matvienko, N. Gubeljak, *Model for Determination of Crack-Resistance of the Pipes*, Patent No. RU 2564696 C, 2015. (in Russian)
92. N. Gubeljak, A. Likeb, Y. Matvienko, *Fracture toughness measurement by using pipe-ring specimens*, Proc. Mater. Sci. **3** (2014), 1934–1940.
93. W. Musraty, B. Medjo, N. Gubeljak, A. Likeb, I. Cvijović-Alagić, A. Sedmak, M. Rakin, *Ductile fracture of pipe-ring notched bend specimens - micromechanical analysis*, Eng. Fract. Mech. **175** (2017), 247–261.

ПРЕГЛЕД ПРИМЕНЕ МИКРОМЕХАНИЧКИХ МОДЕЛА У АНАЛИЗИ ЖИЛАВОГ ЛОМА ЗАВАРЕНИХ СПОЈЕВА

Резиме. Лом заварених спојева је дуго био и још увек је важна тема у истраживачком раду и индустријској пракси, имајући у виду кључну улогу заварених спојева у обезбеђивању безбедног рада и интегритета заварених конструкција. Овај рад садржи преглед примене микромеханичких модела у анализи жилавог лома заварених спојева. Главна предност ових модела, у поређењу са класичним приступом механике лома, је примена локалних величина (напона и деформације) у предвиђању развоја оштећења. Оштећење се квантификује кроз вредност параметра оштећења, који се код жилавог лома металних материјала најчешће доводи у везу са настанком, растом и спајањем шупљина, тј. опис материјала се може довести у везу са реалним понашањем материјала током лома. Већина приказаних истраживања, укључујући она која су објавили аутори овог рада, су урађена на челику као основном материјалу, док се остала односе на легуре алуминијума.

Faculty of Technology and Metallurgy
University of Belgrade
Belgrade
Serbia
marko@tmf.bg.ac.rs

Faculty of Technology and Metallurgy
University of Belgrade
Belgrade
Serbia
bmedjo@tmf.bg.ac.rs

Faculty of Mechanical Engineering
University of Maribor
Maribor
Slovenia

Faculty of Mechanical Engineering
University of Belgrade
Belgrade
Serbia

(Received 17.01.2020.)
(Available online 04.06.2020.)